Reliability Analysis of Numerical Simulation of Sea-Crossing Bridge Deformation Under Wave Forces

LUAN Yuanzhong[1], *YU Jian*[1*], *HU Junwei*[2], *DONG Yue*[1], *GUI Weizhen*[1], *JI Zhaolei*[1]

1.College of Geodesy and Geomatics, Shandong University of Science and Technology, Qingdao 266590, P.R.China;
2.Linyi Huibaoling Iron Ore Limited Company, Linyi 277700, P.R.China

(Received 7 March 2020; revised 15 June 2020; accepted 20 December 2020)

Abstract: To study on the numerical simulation calculation reliability of sea-crossing bridge under complex wave forces, the paper applied GPS deformation monitoring and numerical simulation calculation by researching Qingdao Jiaozhou Bay Sea-Crossing Bridge. The db3 wavelet three-layer decomposition was used on the horizontal movement of the sea-crossing bridge and the wind speed of the waves to analyze their correlation. The complex wave forces value of Qingdao Jiaozhou Bay Sea-Crossing Bridge was loaded on FLAC^{3D} software successfully to make numerical simulation calculation of bridge deformation. Since the accuracy of the GPS deformation monitoring reaches millimeter level, it was used to monitor the exact value of the bridge deformation to judge the reliability of numerical simulation. The relative errors of displacement in X, Y and Z directions were between 33% and 41% through comparison. It could be seen that the numerical simulation error was relatively large, which was mainly due to various environmental factors and the deviation of applied wave forces. However, numerical simulation generally reflects the deformation law of the sea-crossing bridge under complex wave forces, providing an effectively technical support for the safe operation assessment of the sea-crossing bridge.

Key words: sea-crossing bridge; GPS monitoring; three-dimensional deformation; numerical simulation of wave forces; relative error

CLC number: P258 **Document code:** A **Article ID:** 1005-1120(2021)01-0164-09

0 Introduction

In recent years, China has successively built several sea-crossing bridge traffic facilities, such as the Qingdao Jiaozhou Bay Sea-Crossing Bridge, Hangzhou Bay Sea-Crossing Bridge, Shanghai Donghai Bridge, etc. In the complex ocean motion environment[1-3], sea-crossing bridge needs to bear the effects of tidal phenomena and seasonal ocean disasters, such as hurricanes, and other phenomena[4-6] as well as the effects of vehicles. Therefore, it is necessary to comprehensively study the effects of the wave forces on the bridge pier and effectively simulate the deformation of the bridge, which ensures the safe operation and deformation warning of the bridge[7-10].

The traditional monitoring method of bridge vertical displacement is mainly second-order or third-order leveling. Three-dimensional deformation of bridge is mainly monitored by GPS, geo-robots, three-dimensional laser scanner and DinSAR (or PS-DinSAR) measurement technology[11]. These monitoring tools are applied in the deformation monitoring of the sea-crossing bridge, and the measuring accuracy meets the requirements of bridge monitoring. Over the years, a lot of in-depth researches on wave loads have been conducted by scholars at home and abroad and there are many breakthroughs

*Corresponding author, E-mail address: 805339383@qq.com.

How to cite this article: LUAN Yuanzhong, YU Jian, HU Junwei, et al. Reliability analysis of numerical simulation of sea-crossing bridge deformation under wave forces[J]. Transactions of Nanjing University of Aeronautics and Astronautics, 2021, 38(1): 164-172.

http://dx.doi.org/10.16356/j.1005-1120.2021.01.016

in the researches. McIver studied the wave forces on single pile and pile group under the action of irregular waves[12]. Mostafa et al. used the dynamic *p-y* curve to simulate the interaction of pile-soil, and calculated the dynamic response of pile group under wave load through finite element method[13]. Wilson et al. calculated the displacement of the pile body under the action of wave forces by using the dynamic stiffness matrix of the lateral vibration of the continuous system of the single pile offshore platform[14]. It can be seen that relative researches have been carried out about the deformation monitoring of the sea-crossing bridge and simulating the pier deformation under the effect of wave loads. However, some aspects have been barely discussed on evaluating the accuracy of FLAC^{3D} numerical simulation of bridge deformation and analyzing the main factors affecting the numerical simulation[15], based on the observation of GPS deformation.

Therefore, based on the research background of Qingdao Jiaozhou Bay Sea-Crossing Bridge, this paper studied the GPS deformation monitoring and numerical simulation deformation calculation and discussed the real-time relationship between the wave forces and the dynamic deformation of bridge. The quantitative expressions of the wave forces of the pier were determined and loaded on the bridge dynamically in real-time. The difference and relative error between the simulated data of bridge deformation and the measured data of GPS were calculated, so as to evaluate the reliability of the numerical simulation of bridge deformation.

1 Bridge Deformation Monitoring

The action of sea breeze accompanied by waves on bridges is very complex, and its forces are divided into three directions: Vertical, horizontal and torsional directions[16]. A bridge deformation monitoring network has been established at a section of the Qingdao Sea-crossing Bridge, as shown in Fig.1. Q_1, Q_2, Q_3, Q_4, Q_5 and Q_6 are GPS monitoring points arranged for the bridge deck. The length of the bridge section studied is 610 m, and the width is 190 m. Q_2 and Q_5 are located in the perpendicular bisector of the connecting line between the two piers, 40 cm away from the edge. Q_1, Q_2 and Q_3 stand 300 m apart and their connecting line is parallel to the passing direction of the bridge. Q_4, Q_5 and Q_6 are the same as above, and all points are distributed equidistantly on both sides of the bridge deck. Continuously Operating Reference Station was used as the base station to collect the three-dimensional deformation data of the bridge to avoid the conversion error between coordinate systems. WGS-84 coordinate system was used to calculate the three-dimensional deformation value of the bridge. Fig.1 shows two groups of piers of the bridge: D_1 and D_2. Anemometers were installed at the position corresponding to the bridge beam side of Q_1, Q_2, and Q_3 to collect the wind speed value of the monitoring part in real time.

The paper collected nearly 10 000 monitoring data of point Q_2 in 54 days from May 1 to 23 June, 2015. After data processing analysis, the horizontal displacement and the wind speed of the bridge were obtained. The curve graph according to the data is shown in Fig.2.

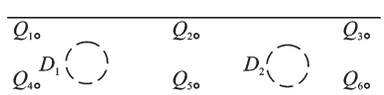

Fig.1 Bridge monitoring point diagram layout

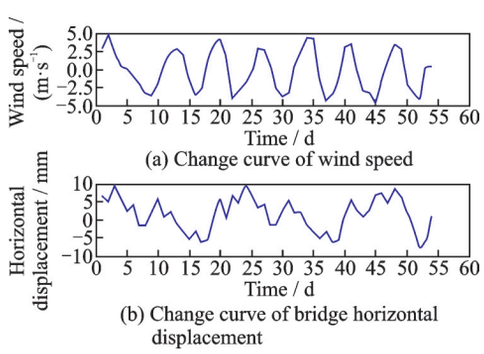

Fig.2 Curve of wind speed and bridge horizontal displacement in *X* direction

2 Wavelet Analysis of Correlation Between Wind Speed and Horizontal Displacement Values

The horizontal displacement in *X* direction (perpendicular to the bridge deck direction) and the

wind speed data were measured at point Q_2 for 54 d. It can be seen from Fig. 2 that there is no obvious correlation between the wind speed and the displacement of the bridge, and the trend of data change is not regular. Wavelet decomposition is performed on the measured wind speed and the horizontal displacement values of the bridge.

Db3 wavelet, coif2 wavelet and Dmey wavelet were applied to deal with the noise processing of the measured deformation data. After comparing the root mean square error (RMSE) and signal to noise ratio (SNR), Dmey wavelet has the least RMSE and the largest SNR. The mean square error of each layer and SNR were compared through db3 wavelet decomposition from layer 1 to layer 5, which indicated that the db3 wavelet three-layer decomposition had the best denoising effect.

RMSE of the variance between the original data and the denoised data is expressed as

$$\mathrm{RMSE}=\{\sum[f(n)-\hat{f}(n)]^2/n\}^{1/2} \tag{1}$$

where n is the size of the signal, $f(n)$ the original signal, and $\hat{f}(n)$ the denoised signal. The smaller the RMSE is, the higher the similarity between the denoised signal and the original signal is, and the better the effect is.

SNR is a commonly used index to measure the noise in data, so it is often used to measure the denoising effect. Its unit is decibel, and it is expressed as

$$\mathrm{SNR}=10\log_{10}(p_s/p_z) \tag{2}$$

where $p_s=\left[\sum_n f^2(n)\right]\Big/n$ is the original signal power and $p_z=\mathrm{RMSE}^2$ is the noise power. The higher the signal-to-noise ratio is, the better the denoising effect is.

In the paper, the RMSE of wind speed is 0.858 9. The RMSE of horizontal displacement is 1.624 7. The SNR of wind speed is 10.268 9. The SNR of horizontal displacement is 9.334 1.

Db3 wavelet was chosen for multi-scale decomposition. There are two purposes of wavelet analysis, one is to denoise the observation values, and the other is to explore the correlation between the horizontal displacement values of bridge and the wind speed. The db3 wavelet three-layer decomposition of wind speed and the details of db3 wavelet decomposition are shown in Fig. 3 and Fig. 4, respectively. The db3 wavelet three-layer decomposition of horizontal displacement values and the details of db3 wavelet decomposition are illustrated in Fig. 5 and Fig. 6, respectively.

According to the correlation coefficient formula, Matlab software is utilized to calculate the corre-

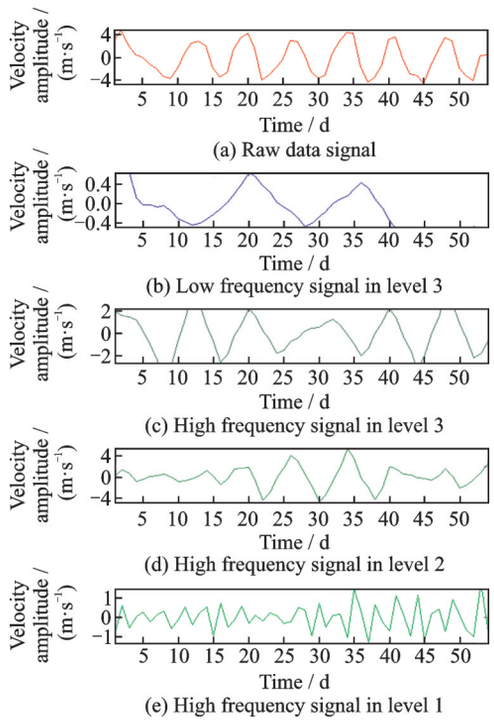

Fig.3 Db3 wavelet three-layer decomposition of wind speed

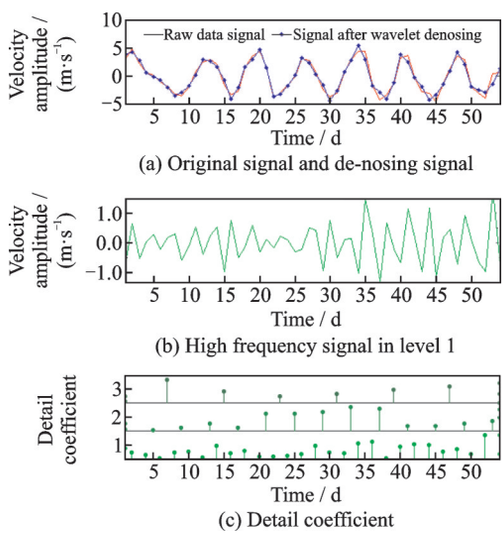

Fig.4 Details of db3 wavelet decomposition of wind speed

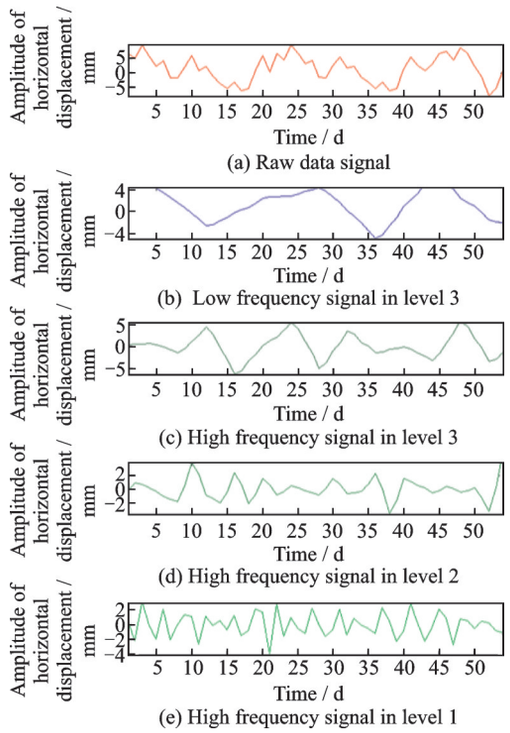

Fig.5 Db3 wavelet three-layer decomposition of horizontal displacement

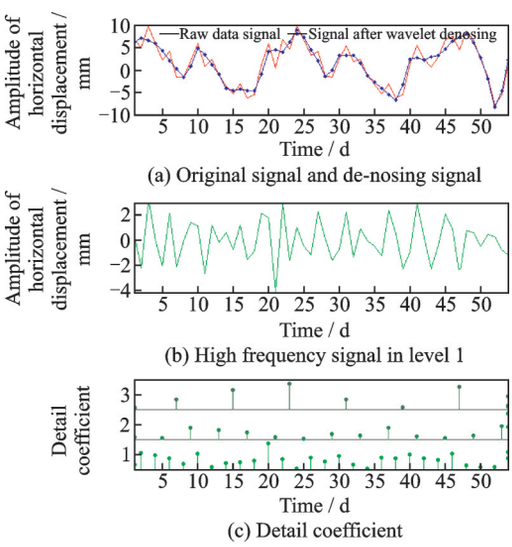

Fig.6 Details of db3 wavelet decomposition of horizontal displacement

lation between the wind speed data after wavelet denoising and the horizontal displacement of bridge after wavelet denoising, shown as

$$r(v_X, u_Y) = \frac{\mathrm{Cov}(v_X, u_Y)}{\sqrt{\mathrm{Var}[v_X]\,\mathrm{Var}[u_Y]}} \tag{3}$$

where v_X is the wind speed after denoising, u_Y the horizontal displacement in X direction after denoising, $\mathrm{Cov}(v_X, u_Y)$ the covariance of v_X and u_Y, $\mathrm{Var}[v_X]$ the variance of v_X, and $\mathrm{Var}[u_Y]$ the variance of u_Y.

The correlation coefficient of wind speed data after wavelet denoising and bridge deformation data after denoising is -0.31. The significance of magnitude of the correlation coefficient is currently inconsistent in the statistical field, but it is generally considered as follows. The correlation coefficients between $0.00 - \pm 0.30$, between $\pm 0.30 - \pm 0.50$, between $\pm 0.50 - \pm 0.80$ and between $\pm 0.80 - \pm 1.00$ belong to micro correlation, real correlation, significant correlation and high correlation, respectively. Accordingly, it can be seen that the wind speed and the horizontal displacement in X direction of bridge are not closely related, and the effect of wind speed does not serve as the main factor for the bridge deformation in a certain range.

By comparing and analyzing Figs.3 and 4 with Figs.5 and 6, it can be seen that by changing wind direction, horizontal displacement varies in X direction, the magnitude of the horizontal displacement changes with the wind speed, and the former lags behind the latter.

Therefore, it is quite essential to monitor the wind speed and its change, which can reflect the deformation of the bridge. Although the specific relationship between wind speed and horizontal displacement in X direction is not identified, results indicate that only keeping the wind speed in a certain range can guarantee the safety of bridge.

3 Calculation of Wave Forces

The wave forces is composed of drag force $k_2 u|u'|$ and wave acceleration inertial force $k_1 u'$, calculated by the Morison equation

$$f = k_2 u|u'| + k_1 u' \tag{4}$$

where $k_1 = c_M \dfrac{RA}{g} = c_M \dfrac{R\pi D^2}{4g}$, $k_2 = c_D \dfrac{D}{2g}$, c_M is the inertial force coefficient, c_D the drag force coefficient, A the cross-sectional area of the bridge pier cylinder, D the diameter of the cylinder, R the bulk density of the seawater, and g the acceleration of gravity.

Pier's wave force is calculated as an isolated building because of small size, and the ratio of the

width of the wavefront to the wavelength is $D / L < 0.2$. The average high tide level is 3.41 m and the wave height is 1.49 m, corresponding to effective wave period $T=60$ s and wavelength 52.8 m.

The wave force of each pile in a group is different from that of a single pile, which is mainly caused by the phase difference and the flow field interference between the piles in the group[17]. In this paper, only the pile group coefficient caused by phase difference is considered, which is defined as

$$K=\frac{\left|\sum_{i=1}^{n}F_i(t)\right|_{\max}}{\sum_{i=1}^{n}\left|F_i(t)\right|_{\max}} \tag{5}$$

where $\left|\sum_{i=1}^{n}F_i(t)\right|$ is the sum of wave force of each pile at time t, and $\left|F_i(t)\right|_{\max}$ the maximum wave force on the i-th pile.

According to the relevant regulations of the seaport hydrological code, when calculating the total wave force on each pile at the same time, it should be multiplied by the group pile coefficient K, which is 0.866 according to the aforementioned formula.

According to the Morison equation, the program is compiled in Matlab language to calculate the wave forces of particles on water surface and the time-history curve is shown in Fig.7.

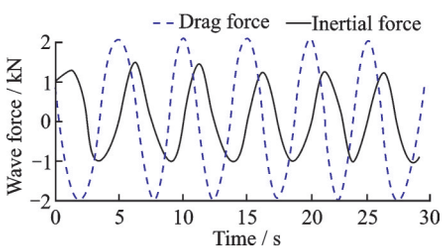

Fig.7 Time-history curves of wave force

4 Equation of Wave Particle Motion

Applying the theory of linear wave superposition, the vertical displacement of sea wave can be decomposed into an infinite superposition of simple waves with frequency=w_n, amplitude=a_n and initial phase=ε_n. In this way, the formula of discrete and continuous vertical displacement fluctuation can be obtained as:

Discrete vertical displacement fluctuation is

$$\zeta(t)=a_n\cos(k_nx-w_nt+\varepsilon_n)$$

Continuous vertical displacement fluctuation is

$$\zeta'(t)=\int_0^{\infty}\sqrt{2G_\zeta(w)\,\mathrm{d}w}\cos(kx-wt+\varepsilon)$$

According to the law of wave particle motion, the horizontal velocity and acceleration of the particles can be expressed as:

Horizontal velocity of the particles is

$$u_{\mathrm{H}}=\sum_{n=1}^{\infty}a_nw_n\frac{\mathrm{ch}\,k_n(z-d)}{\mathrm{sh}\,k_nd}\cos(k_nx-w_nt+\varepsilon_n)$$

Horizontal acceleration of the particles is

$$\alpha=\sum_{n=1}^{\infty}a_nw_n^2\frac{\mathrm{ch}\,k_n(z-d)}{\mathrm{sh}\,k_nd}\sin(k_nx-w_nt+\varepsilon_n)$$

where $\varepsilon, \varepsilon_n$ are the random variables; $G_\zeta(w)$is the spectrum; λ the wavelength; k the wave number, $k=\frac{2\pi}{\lambda}$; $w=\frac{2\pi}{T}$, T the period and w the circular frequency.

5 Numerical Simulation of Bridge Deformation

5.1 Model establishment

The studied section of Jiaozhou Bay Bridge is a pile group foundation with 24 root piles in total. Each pile has a length of 70 m, a diameter of 2.5 m, and a pile spacing of 6.25 m. The cushion cap is a round chamfered octagon with a length of 42 m, a width of 23.25 m and a thickness of 6 m, as shown in Fig.8. The modeling method is to build a single pile model first, and then build a group pile model[18].

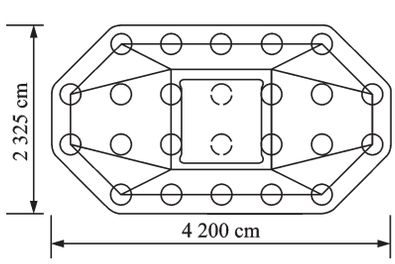

Fig.8 Top view of pile group foundation

Radcylinder is chosen to build the soil mass around single piles, and then cylinder is selected to build single piles. During the process of modeling, mirror reflect is used to obtain the single pile model.

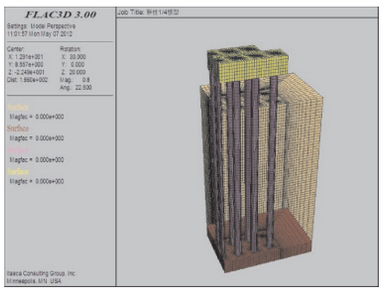

Fig.9 Rendering of pile group foundation model

Since the force acting on the pile body is axisymmetric, the 1/4 model of the actual shape is selected for simulation. The basic unit of pile group is single pile and the commands such as reflect, copy and merge should be used in the modeling of pile group. The model is shown in Fig.9.

5.2 Numerical simulation

The Coulomb shear model is adopted for the contact surface of the model. As pile group and cap are both linear elastic bodies, elastic material is used in simulation. The plastic material is selected for the soil around the pile and Mohr Coulomb constitutive model is used. Numerical simulation parameters are shown in Table 1.

Table 1 Parameters of model materials

Soil layer	Density/ ($kg \cdot m^{-3}$)	Cohesive force/kPa	Friction angle/ (°)	Poisson's ratio	Modulus of elasticity/MPa	Bulk modulus/MPa	Shear modulus/MPa
Silt/muddy clay	1 900	20	18	0.3	20	1.67	0.77
(Sub) clay	2 000	10	10	0.3	24	20.00	9.00
Medium coarse sand	2 100	0	32	0.3	40	33.30	15.40
Bedrock	2 500	0	55	0.2	50 000	27 778.00	20 833.00
Pile (concrete C35)	2 500			0.2	25 000	13 889.00	10 417.00

Considering the influence of the superstructure on the pier, the upper gravity load is first applied on the cap[19]. What is usually loaded in FLAC^{3D} simulation is the stress, and the stress on the surface of the cap should be obtained by simple calculation, where the stress loaded is the load carried per unit area. Key monitoring points are set in the command flow. During the process of numerical simulation, the sinking of the foundation piles of the following locations ought to be monitored respectively: In the middle of the pile cap, at the top of the side pile cap along the bridge and at the top of the lateral side pile cap.

The displacement changes at different positions of piles are recorded. The center pile in the pile group foundation is selected as the analysis object, and the displacement changes are recorded at different positions on the upper, middle and lower of the central foundation pile. The vertical displacement nephogram of pile group under the gravity load of superstructure is shown in Fig.10, and that of pier is shown in Fig.11.

On the basis of the gravity load of the superstructure, the wave force load and wind load are applied. The measured wind speed of the bridge section is low, which affects less on the bridge deformation. Besides, this paper focuses on the effect of the wave force, which gives rise to the bridge deformation. Therefore, the wind load and wave force load are considered as a comprehensive action. According to the action law, i.e., wave force time-

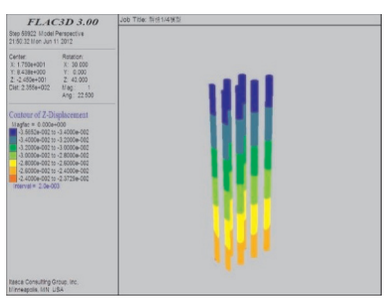

Fig.10 Nephogram of vertical displacement

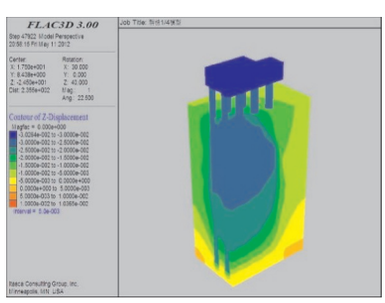

Fig.11 Nephogram of vertical displacement of pier

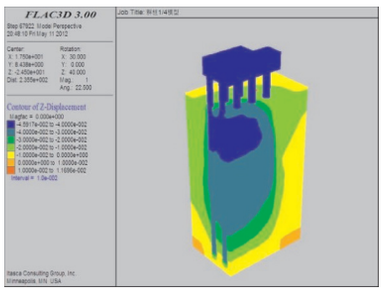

Fig.12 Nephogram of vertical displacement of pier

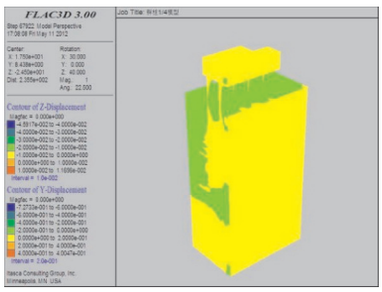

Fig.13 Nephogram of horizontal displacement of pier

history curve shown in Fig.7 and combined with the measured wind speed value, the vertical and horizontal displacement nephograms of wave force load and wind load continuously applied to the pier at a certain time are shown in Fig.12 and Fig.13.

The 3-D displacement values of pier of eight equally spaced discrete moments under the action of periodic wave force is shown in Table 2.

Table 2 Numerical simulation of deformation at different moments

Displacement	1	2	3	4	5	6	7	8
X direction/mm	0.6	1.9	−3.5	3.5	2.2	−5.0	1.6	6.1
Y direction/mm	−3.8	5.5	4.1	−7.8	3.3	0.0	−0.8	0.4
Z direction/mm	4.3	9.0	−2.1	8.0	3.5	−4.7	2.2	3.3

6 Comparison of GPS Observed Values and Numerical Simulation Values

Comparing the above three-dimensional displacement values of the bridge pier and GPS deformation observed values in the corresponding time, the displacement differences are shown in Table 3.

It can be seen from Table 3 that the average relative error of displacement difference between GPS deformation observation and numerical simulation is 33% in *X* direction, 41% in *Y* direction and 35% in *Z* direction. The displacement of the bridge pier does not represent the displacement of the bridge. This is only an approximate numerical method. In fact, the displacement of the bridge is caused by such environmental factors as wind, wave, current and so on. At the same time, there are errors in applying wave forces. The results of the numerical simulation basically reflect variation law of the three-dimensional displacement of the pier, which provides a more reliable technical means for the safety assessment of the bridge in response to the hurricane and other marine disasters.

Table 3 Comparison of 3-D displacement between measurement and simulation values at different moments

Moment	*X* direction displacement / mm			*Y* direction displacement / mm			*Z* direction displacement / mm		
	φ_m	φ_s	φ_{da}	φ_m	φ_s	φ_{da}	φ_m	φ_s	φ_{da}
1	1.9	0.6	1.3	−2.6	−3.8	1.2	5.5	4.3	1.2
2	0.5	1.9	1.4	1.8	5.5	2.3	10.3	9.0	1.3
3	−2.5	−3.5	1.0	6.1	4.1	2.0	−4.1	−2.1	2.0
4	5.6	3.5	2.1	−6.4	−7.8	1.4	6.6	8.0	1.4
5	3.3	2.2	1.1	5.6	3.3	2.3	5.0	3.5	1.5
6	−2.9	−5.0	2.1	1.1	0.0	1.1	−2.5	−4.7	2.2
7	2.2	1.6	0.6	−1.8	−0.8	1.0	3.6	2.2	1.4
8	8.4	6.1	2.3	1.6	0.4	1.2	5.4	3.3	2.1

φ_m: Measured value; φ_s: Simulation value; φ_{da}: Absolute value of difference.

7 Conclusions

Based on the GPS deformation monitoring of Qingdao Jiaozhou Bay Sea-Crossing Bridge, this paper calculates the wave forces on the pier and studies the numerical simulation of the bridge deformation under the dynamic loading of the wave forces. The conclusions are as follows:

(1) The db3 wavelet three-layer decomposition was performed respectively on the GPS measured values, the horizontal displacement values of bridge and the corresponding wind speed values. The results indicate that the deformation of the sea-crossing bridge is related to the wind speed, and the displacement is proportional to the wind speed. With the change of wind direction, horizontal displacement varies in X direction, and the change of the displacement lags behind that of the wind speed.

(2) According to the wave motion parameters and Morison equation, the pile coefficient caused by the phase difference was introduced to obtain the time-history curve of the wave forces of the pier water surface particles.

(3) According to the mechanical parameters of the bridge pier, FLAC^{3D} numerical simulation software was used to make the numerical simulation calculation of the dynamic loading of bridge pier in real-time wave forces after the gravity load of the superstructure considered. So the real-time dynamic deformation of sea-crossing bridge was obtained.

(4) Through the comparative analysis between the measured values and the numerical simulation deformation values of the sea-crossing bridge, the relative error of displacement in X direction, Y direction and vertical direction is between 33% and 41%, indicating that the error of the numerical simulation is relatively large. In addition to other environmental factors, the real-time dynamic application of wave force is one of the main factors affecting the accuracy of numerical simulation. Therefore, it is of vital importance to calculate the wave forces accurately.

The numerical simulation, however, basically reflects the deformation law of the sea-crossing bridge, which provides the technical support for its safety assessment.

References

[1] PEACHY D R. Modeling wave and surf[J]. Computer Graphics, 1986, 20(3): 65-74.

[2] FOURNIER A, REEVES W T. A simple model of ocean waves[J]. Computer Graphics, 1986, 20(4): 75-84.

[3] WANG Changbo, WANG Zhangye, JIN Jianqiu. Real-time simulation of ocean wave based on cellular automata[C]//Proceedings of 8th International Conference on CAD/Graphics. Macao, China: IEEE, 2003.

[4] YANG Huaiping, SUN Jiaguang. Wave simulation based on ocean wave spectrums[J]. Journal of System Simulation, 2002, 14: 1175-1179. (in Chinese)

[5] TESSENDORF J. Simulating ocean water[C]//Proceedings of ACM SIG-GRAPH. [S.l.]: ACM Press, 1999.

[6] ZHU Yanrong. Wave dynamics in ocean engineering [M]. Tianjin: Tianjin University Press, 1991. (in Chinese)

[7] ZHAO Xin, LI Fengxia, CHEN Hongmin, et al. Ocean wave simulation near the seashore[J]. Journal of Beijing Institute of Technology, 2009, 18(2): 181-185.

[8] WANG Jianbo. Application of wavelet transform in data processing of bridge deformation monitoring[D]. Shandong: Shandong University of Science and Technology, 2011. (in Chinese)

[9] LUAN Yuanzhong, CAO Dingtao, XU Lenian, et al. Deformation observation and dynamic prediction[M]. Beijing: Meteorological Press, 2001. (in Chinese)

[10] LIU Tao. Practical wavelet analysis[M]. Beijing: National Defense Industry Press, 2006. (in Chinese)

[11] LUAN Yuanzhong, LUAN Hengxuan, MA Depeng. Wavelet denoise and chaos prediction of bridge deformation data[J]. Geodetic Survey and Earth Dynamics, 2013, 33(5): 133-135. (in Chinese)

[12] MCIVER P, EVANS D V. Approximation of wave forces on cylinder arrays[J]. Applied Ocean Research, 1984, 6(2): 101-107.

[13] MOSTAFA Y E, NAGGAR M H E. Response of fixed offshore platforms to wave and current loading including soil-structure interaction[J]. Soil Dynamics &

Earthquake Engineering, 2004, 24(4): 357-368.
[14] WILSON D W, BOULANGER R W, KUTTER B L. Observed seismic lateral resistance of liquefying sand[J]. Journal of Geotechnical & Geoenvironmental Engineering, 2000, 126(10): 898-906.
[15] HUANG Peiji, HU Zejian. Fitting model of wind wave spectrum in Jiaozhou Bay[J]. Advances in Marine Science, 1987(3): 1-7. (in Chinese)
[16] FANG Yiyuan, WANG Huzhuang, CHEN Kangsheng. Computer simulation research of one-dimensional wave spectrum SAR imaging[J]. Journal of Telemetry, Tracking and Command, 1995(5): 25-30. (in Chinese)
[17] WU Anjie, YANG Wanli. Numerical study of pile group effect on the hydrodynamic force on a pile of sea-crossing bridges during earthquakes[J]. Ocean Engineering, 2020, 199: 106999.
[18] CHE Xiaojun. Simulation modeling of dynamic characteristics of sea crossing bridge under wind invasion[J]. Journal of Coastal Research, 2018, 83(1): 93-97.
[19] LUO Junhui, LIU Xianlin, MI Decai, et al. Intelligent dynamic response of Guangxi marine soft foundation under traffic load[J]. Journal of Intelligent and Fuzzy Systems, 2019, 37(4): 1-8.

Acknowledgement This work was supported by the Natural Science Foundation of Shandong Province (No. ZR2020MD024).

Authors Prof. **LUAN Yuanzhong** received the B.S. degree in mine surveying from Shandong University of Mining and Technology in 1985 and he obtained the M.S. degree in engineering surveying from Central South University of Technology in 1994. Then, he graduated with Ph.D. degree in geodesy and surveying engineering from Tongji University in 2004, and completed the post doctoral research.

Mr. **YU Jian** obtained the B.S. degree in surveying and mapping engineering from Shandong University of Science and Technology (SDUST) in 2018, and then studied for M.S. degree in Geodesy and Surveying Engineering of SDUST from 2018 to now.

Author contributions Prof. **LUAN Yuanzhong** provided the main ideas and technical route of the paper. Mr. **YU Jian** analyzed the data and wrote the paper. Mr. **DONG Yue** conducted the wavelet analysis. Mr. **GUI Weizhen** conducted the simulation. Mr. **JI Zhaolei** and Mr. **HU Junwei** reviewed the paper and provided advices. All authors approved the submission.

Competing interests The authors declare no competing interests.

(Production Editor: SUN Jing)

波浪力作用下跨海大桥变形数值模拟的可靠性分析

栾元重[1],于 健[1],胡军伟[2],董 岳[1],桂维振[1],纪赵磊[1]
(1.山东科技大学测绘与空间信息学院,青岛 266590,中国;
2.临沂会宝岭铁矿有限公司,临沂 277700,中国)

摘要:针对跨海大桥在复杂海浪力作用下数值模拟计算的可靠性问题,以青岛胶州湾跨海大桥为研究背景,开展了GPS变形监测与数值模拟计算。对监测的跨海大桥水平移动与海浪风速值进行了db3小波三层分解,分析了桥梁水平变形值与风速相关关系。将青岛胶州湾跨海大桥计算的复杂海浪作用力量值,成功地加载于FLAC3D软件,实现了桥梁变形的数值模拟计算。由于GPS变形监测精度可达到毫米级,故以其为桥梁变形准确值,判断数值模拟可靠性。经比较,X方向、Y方向及Z方向位移相对误差介于33%~41%之间,可见数值模拟误差较大,这主要是由于多种环境因素影响以及施加海浪力偏差引起的。但数值模拟总体上反映了跨海大桥在复杂的海浪力作用下的变形规律,为准确地评估跨海大桥安全运营提供了一种有效的技术支撑。

关键字:跨海大桥;GPS监测;三维变形;海浪力数值模拟;相对误差